HHS Public Access

Author manuscript

Science. Author manuscript; available in PMC 2022 November 07.

Published in final edited form as:

Science. 2022 September 23; 377(6613): 1399–1406. doi:10.1126/science.abn0910.

Liver-heart cross-talk mediated by coagulation factor XI protects against heart failure

Yang Cao[1], **Yuchen Wang**[1], **Zhenqi Zhou**[2], **Calvin Pan**[1], **Ling Jiang**[3], **Zhiqiang Zhou**[1], **Yonghong Meng**[1], **Sarada Charugundla**[1], **Tao Li**[3], **Hooman Allayee**[4], **Marcus M. Seldin**[5], **Aldons J. Lusis**[1,6,7,*]

[1]Department of Medicine, Division of Cardiology, University of California, Los Angeles, CA 90095, USA.

[2]Division of Endocrinology, Diabetes and Hypertension, Department of Medicine, University of California, Los Angeles, CA 90095, USA.

[3]Department of Anesthesiology, Laboratory of Mitochondria and Metabolism, West China Hospital of Sichuan University, Chengdu 610041, China.

[4]Departments of Population and Public Health Sciences and Biochemistry and Molecular Medicine, University of Southern California Keck School of Medicine, Los Angeles, CA 90089, USA.

[5]Department of Biological Chemistry and Center for Epigenetics and Metabolism, University of California, Irvine School of Medicine, Irvine, CA 92697, USA.

[6]Department of Human Genetics, University of California, Los Angeles, CA 90095, USA.

[7]Department of Microbiology, Immunology and Molecular Genetics, University of California, Los Angeles, CA 90095, USA.

Abstract

Tissue-tissue communication by endocrine factors is a vital mechanism for physiologic homeostasis. A systems genetics analysis of transcriptomic and functional data from a cohort of diverse, inbred strains of mice predicted that coagulation factor XI (FXI), a liver-derived protein, protects against diastolic dysfunction, a key trait of heart failure with preserved ejection fraction. This was confirmed using gain- and loss-of-function studies, and FXI was found to activate the bone morphogenetic protein (BMP)–SMAD1/5 pathway in the heart. The proteolytic activity of

*Corresponding author. jlusis@mednet.ucla.edu.

Author contributions: Y.C., M.M.S., and A.J.L. designed the experiments. Y.C., Y.W., Z.Z., L.J., Z.Z., Y.M., S.C., and T.L. performed the experiments. Y.C., L.J., M.M.S., and C.P. analyzed raw data. Z.Z., H.A., M.M.S., and A.J.L. reviewed the data and made substantial contributions to improving the studies. Y.C. and A.J.L. wrote the manuscript, which was reviewed by all authors.

Competing interests: The authors declare no competing interests.

Data and materials availability: All data supporting the conclusions in this manuscript can be found in the main text or the supplementary materials. RNA-Seq data were deposited to the Gene Expression Omnibus (GEO) database (https://www.ncbi.nlm.nih.gov/geo/) under accession number GSE200496. The R script used to perform the volcano plots and PCA plot are available at Zenodo (44).

SUPPLEMENTARY MATERIALS

science.org/doi/10.1126/science.abn0910

FXI is required for the cleavage and activation of extracellular matrix–associated BMP7 in the heart, thus inhibiting genes involved in inflammation and fibrosis. Our results reveal a protective role of FXI in heart injury that is distinct from its role in coagulation.

Tissue-tissue cross-talk by endocrine factors, including secreted proteins (1), is a vital mechanism to maintain proper physiologic homeostasis. The heart and the liver display multifaceted interactions (2), and in clinical practice it is common to observe heart diseases affecting the liver and vice versa (3). For instance, nonalcoholic fatty liver disease increases the risk for heart failure with diastolic and systolic dysfunction (4, 5). On the basis of these observations, we hypothesized that secreted proteins may mediate communication between liver and heart. We screened for such endocrine factors using a “systems genetics” approach that integrates natural variation for physiological and clinical traits with global transcriptomics data in cohorts of genetically diverse mice. In our studies, we used a resource consisting of ~100 diverse, inbred strains of mice called the Hybrid Mouse Diversity Panel (HMDP) (6). Among several candidates that were identified was coagulation factor XI (FXI), a protein produced exclusively by liver.

We validated several of these factors in a mouse model of a common form of heart failure, heart failure with preserved ejection fraction (HFpEF). We reasoned that we were more likely to see an effect if the heart was stressed. HFpEF is characterized by diastolic dysfunction and preserved ejection fraction, which is distinct from heart failure with reduced ejection fraction (HFrEF) (7). HFpEF accounts for half of all cases of heart failure and is associated with multiple comorbidities, including diabetes, hypertension, and restrictive cardiomyopathies (8, 9). In HFpEF, chronic systemic inflammation and metabolic disorders affect not only the myocardium, but also other organs such as the kidneys, lungs, and skeletal muscles. However, little is known about the molecular mechanisms underlying impaired cardiac relaxation and how other organs interact with the heart to regulate the pathophysiology of HFpEF.

We chose to follow up on FXI, which was particularly interesting because not only did it perturb gene expression in the heart, but it also affected diastolic function. In the mouse model of HFpEF, mice overexpressing FXI in liver showed improved diastolic function, whereas FXI-knockout mice were sensitized for diastolic dysfunction. We identified potential pathways by which FX1 affects diastolic function by examining differential gene expression in response to changes in FXI levels. FXI overexpression activated the bone morphogenetic protein (BMP)–SMAD1/5 pathway in the heart. The action of FXI on the heart requires proteolytic activity, because point mutations in its catalytic domain eliminated the effects on BMP signaling and heart function. BMP7 is secreted as an inactive precursor that binds to the extracellular matrix, and our results indicate that it is cleaved by FXI, releasing the active growth factor from the prodomain. We also provide evidence that FXI has a similar function in humans. Our results identify FXI as an endocrine factor that influences heart function, and this is distinct from its role in coagulation.

Results

Systems genetics screening for potential regulators of liver-heart cross-talk

To identify endocrine circuits mediating liver-heart cross-talk (10), we took advantage of a recently developed bioinformatics approach that uses natural variation to identify correlations between tissues. For this, we used a panel of 100 diverse inbred mouse strains in the HMDP (6, 11). Global transcriptomic data from the heart and the liver were generated across all 100 inbred strains and used to detect the correlations between secreted proteins from the liver and their downstream effects on the heart (Fig. 1A). By assessing the strength of cross-tissue predictions, we generated a list of potential liver-heart mediators (Fig. 1B and table S1). The top-ranked candidates included *Igfbp7, Lipc, Emilin1, Lgals9, St6gal1, Ghr, Crlf2, Lcat*, and *F11*. This list revealed several previously described mediators with consistent functions. For instance, insulin-like growth factor-binding protein-7 (*Igfbp7*) has been reported to be correlated with diastolic function in HFrEF and HFpEF patients (12).

FXI protects against diastolic dysfunction, fibrosis, and inflammation in a mouse model of HFpEF

On the basis of their specific expression in the liver, data from the literature, and functional annotation, we selected *Hgfac, C8g*, and *F11* as candidate mediators of liver-heart communication (Fig. 1B). To determine whether these factors have clinically relevant effects on the heart, we examined them in a mouse model of HFpEF, which is characterized by diastolic dysfunction. We overexpressed these genes individually in the livers of C57BL/6J male mice with an adeno-associated virus serotype 8 (AAV8) vector carrying target genes or green fluorescent protein (GFP) control and directed by the liver-specific thyroid hormone-binding globulin promoter (fig. S1A). After AAV8 injection, mice were subjected to a "two-hit" HFpEF model induced by a combination of high-fat diet (HFD) and inhibition of nitric oxide synthase using Nω-nitrol-arginine methyl ester (l-NAME) (13), followed by assessment of cardiac functions (fig. S1B). After 7 weeks of HFD + l-NAME feeding, mice developed heart failure phenotypes that recapitulated the clinical symptoms of HFpEF, including diastolic dysfunction [increased E/A ratio, E/e′ ratio, left ventricular (LV) mass, heart weight, and lung weight], metabolic disorders (increased body weight, fat mass, plasma lipids, and glucose intolerance), exercise intolerance (reduced running distance), and preserved LV ejection fraction (LVEF) (fig. S1, C to N).

We observed that when overexpressed, liver-derived hepatocyte growth factor activator (HGFAC) increased LV mass and complement C8 gamma chain (C8G) decreased heart weight in the model of HFpEF (figs. S2 and S3). However, we focused on the other top candidate, FXI, because it had additional effects on several HFpEF traits, including diastolic function. FXI acts downstream of FXII (14, 15) and triggers the middle phase of the intrinsic pathway of blood coagulation by activating FIX. Like HGFAC and C8G, FXI is also exclusively expressed in the liver (Fig. 1C and fig. S4, A and B). Furthermore, on the basis of associations with heart transcript levels in the HMDP, FXI was predicted to be strongly correlated with critical pathways in the heart and a number of clinical traits related to HFpEF (Fig. 1D and fig. S4C). In addition, human genome-wide association studies (GWAS) revealed that genetic loci encompassing the *F11* gene were associated with the total

cholesterol and BMP7 levels (Fig. 1E and tables S2 and S3) (16). These data suggested a potential role of FXI in heart failure.

We observed reduced plasma FXI in the mice on HFD + l-NAME relative to those given a chow diet (fig. S4, D and E). We then induced the HFpEF model in 30 genetically diverse, inbred strains of mice, a subset of HMDP, to examine the association between plasma FXI and diastolic dysfunction in the context of naturally occurring variation. We found that FXI levels were inversely correlated with diastolic dysfunction after feeding the HFpEF diet (Fig. 2A). Taken together, these results suggest that FXI may protect against diastolic dysfunction.

We then directly validated the function of FXI in the HFpEF model using overexpression. C57BL/6J male mice injected with AAV8-*GFP* or AAV8-*F11* were subjected to chow diet or HFD + l-NAME for 7 weeks (fig. S1B). After AAV8 injection, *F11* expression was elevated in the liver and FXI protein was increased in the plasma (Fig. 2, B and C, and fig. S5, A and B). We injected sufficient virus to increase FXI protein levels only modestly (about 1.4-fold) to avoid nonphysiological artifacts. Plasma alanine transaminase levels were not significantly changed ($P = 0.29$) by FXI overexpression, suggesting no deleterious effects on the liver from overexpression (fig. S5C). FXI protein was not detected in the heart, confirming the specificity of AAV8 to target the liver and supporting the concept that FXI is an endocrine factor produced by the liver that affects the heart (fig. S5D). Mice receiving AAV8-*F11* had lower body weight and fat mass after HFpEF compared with those receiving AAV8-*GFP* (fig. S5E). Blood pressure was not affected by FXI (fig. S5F). Consistent with our genetic results in the HMDP, FXI overexpression decreased E/A ratio, E/e′ ratio, heart weight, and lung weight in the HFpEF model while preserving LVEF, indicating an improvement in diastolic function (Fig. 2, D to I, and fig. S5G). Running distance was also improved by FXI overexpression, indicating that FXI ameliorates exercise intolerance in HFpEF (Fig. 2J). FXI overexpression also had beneficial metabolic effects on fat mass and plasma lipid levels (fig. S6, A to D) but not on glucose tolerance (fig. S6, E to G).

To test whether FXI overexpression affects blood coagulation, we measured blood thrombin-antithrombin complexes in mice with GFP or FXI overexpression and found that they were not significantly changed ($P = 0.79$) in mice receiving AAV8-*F11* versus AAV8-*GFP* (Fig. 2K), suggesting that the coagulation system was not affected by FXI overexpression. It has been found that mean platelet volume, reflecting the size and activity of platelets, is increased in decompensated heart failure patients and correlates with disease severity, serving as an independent predictor of 6-month mortality after decompensation (17). We observed a small but significant increase of mean platelet volume upon HFpEF development ($P < 0.05$), and FXI overexpression reversed it ($P < 0.01$) (fig. S6H). FXI overexpression significantly reduced circulating inflammatory cells ($P < 0.05$) and cytokine levels [interleukin β (IL-β) and IL-6, $P < 0.05$; interferon γ, $P < 0.01$] in the HFpEF model (fig. S6, I and J). Moreover, the expression of inflammatory genes in the heart was also reduced by FXI overexpression (Fig. 2L and fig. S6K). When mice were maintained on a chow diet, the number of blood immune cells was not changed by FXI overexpression (fig. S6L).

To further test whether the cardiac infiltration of inflammatory cells was attenuated by FXI, we performed multiplex immunohistochemistry using antibodies against macrophages (F4/80), T cells (CD3), monocytes (Ly6C), and granulocytes (Ly6G). We observed significantly decreased inflammatory cells (F4/80, $P < 0.0001$; CD3, $P < 0.05$; Ly6C and Ly6G, $P < 0.01$) in heart tissue from FXI-overexpressing mice versus GFP-overexpressing mice (Fig. 2, M and N), suggesting that FXI overexpression reduced inflammation in heart tissue in the HFpEF model. In addition, FXI overexpression also decreased fibrosis in the heart (Fig. 2, O and P).

FXI activates the BMP-SMAD1/5 pathway in cardiomyocytes

To investigate the molecular mechanism underlying the impact of FXI on the heart, we performed RNA sequencing (RNA-Seq) of the mice with FXI versus GFP overexpression in heart and adipose. Compared with GFP controls, 124 genes in the heart were significantly changed (adjusted $P < 0.05$) by FXI overexpression (fig. S7, A to C). Differentially expressed genes were enriched in pathways related to circadian rhythm, cardiac muscle contraction, inflammation, focal adhesion, the phosphatidylinositol 3-kinase (PI3K)–Akt pathway, and insulin signaling (fig. S7D). In contrast to the heart, only six genes in white adipose tissue were significantly changed (adjusted $P < 0.05$) by FXI overexpression (fig. S7E). *Tcap* (Titin-cap), and *Lrrc10* (Leucine-rich repeat-containing 10), two genes involved in cardiac myofibril assembly and cardiac muscle tissue morphogenesis (2), were increased in the heart tissue of FXI-overexpressing mice (fig. S7, F and G).

To identify pathways perturbed by FXI, we again turned to the HMDP. Because we had performed global transcriptomics in the heart as well as the liver in all 100 strains, we could identify heart genes in which expression was correlated with the expression of FXI in the liver. On the basis of this, we examined the protein or RNA levels of the predicted pathways (Fig. 1E) and RNA-Seq (fig. S7), including the PI3K-Akt, nuclear factor κB, SMAD, and tumor necrosis factor-α (TNF-α) pathways (Fig. 3A and fig. S8A). We observed that members of the BMP pathway were correlated with FXI expression, and the link to BMP was supported by data from human GWAS (discussed below). Consistent with this, our overexpression studies showed that FXI induced an increase in SMAD1/5 phosphorylation and a decrease in TNF-α in the heart but not in other tissues (Fig. 3A and fig. S8, A to H), suggesting activation of the BMP-SMAD1/5 pathway and a decrease of inflammation in the heart. To test whether nuclear p-SMAD1/5 was also increased, we isolated the nuclear fraction from the same heart tissue and observed that it was significantly induced in the FXI overexpression group relative to GFP controls ($P < 0.0001$) (fig. S8I). We injected C57BL/6J male mice with saline control or mouse FXI protein and, after 2 hours, observed the phosphorylation of SMAD1/5 in the heart but not in other tissues, supporting the tissue-specific activation of the BMP-SMAD1/5 pathway by FXI (fig. S8, J to M). Plasminogen activator inhibitor-1 (PAI-1) was comparable in the hearts receiving AAV8-*F11* relative to those receiving AAV8-*GFP* (fig. S8A). However, FXI overexpression reversed the expression of the fibrotic and inflammatory genes *Col5a1, Col5a3, Adam19, IL1β, IL6*, and *Tnf* in the heart but not in other tissues examined, consistent with the observed decrease in fibrosis and inflammation in the heart (Fig. 3B and fig. S8, N and O).

To determine the localization of p-SMAD1/5, we stained p-SMAD1/5 and the markers of cardiomyocytes (troponin I), fibroblasts (vimentin), macrophages (CD68), and endothelial cells (CD31) in the heart after FXI overexpression. p-SMAD1/5 was colocalized with troponin I, but not with other markers (fig. S9), suggesting that p-SMAD1/5 was mainly activated in cardiomyocytes. To directly test whether FXI protein activates the BMP-SMAD1/5 pathway in cardiomyocytes, we incubated neonatal rat ventricular myocytes (NRVMs), human embryonic stem cell–induced cardiomyocytes, and other cell lines with control medium or medium containing human activated FXI protein (FXIa) in the presence of phenylephrine for 24 hours. We observed that FXIa increased the phosphorylation of SMAD1/5 and decreased the expression of *Nppa, Nppb, Col5a3*, and *Adam19* in NRVMs and human embryonic stem cell–induced cardiomyocytes but not in other cell types (Fig. 3, C and D, and fig. S10).

The above experiments were performed with male mice and we were interested in determining whether the results were similar with females. C57BL/6J female mice injected with AAV8-*GFP* or AAV8-*F11* were subjected to HFD + l-NAME for 7 weeks (fig. S11A). After AAV8 injection, *F11* expression was increased in the liver (fig. S11B). We observed similar effects of FXI in female mice, including decreased body mass, decreased inflammatory cells in the blood, reduced plasma lipids, increased SMAD1/5 phosphorylation, improved diastolic function, and reduced heart weight and lung weight (fig. S11, C to N). By contrast, blood pressure was comparable between the FXI and GFP groups (fig. S11O).

To determine whether the effects of FXI that we observed were specific to the HFpEF model, we examined a “multi-hit” HFpEF model induced by the combination of aging, HFD, and angiotensin II (18). Aged C57BL/6J male mice were injected with AAV8-*GFP* or AAV8-*F11* and then fed a HFD for 12 weeks. After 8 weeks of HFD, mice were infused with angiotensin II for 4 weeks (fig. S12A). *F11* mRNA was increased in the liver by AAV8-*F11* compared with AAV8-*GFP* controls (fig. S12B). Similar to the beneficial effects in the “two-hit” HFpEF model, we observed significant improvement in diastolic function and related traits in FXI-overexpressing mice relative to GFP-overexpressing mice, including reduced body mass ($P < 0.05$) (fig. S12C) and improved diastolic function as measured by lower E/A ratio ($P < 0.05$), lower E/e′ ratio ($P < 0.001$), and lower LV mass ($P < 0.05$) (fig. S12, D to H). In addition, FXI-overexpressing mice exhibited reduced heart weight and plasma total cholesterol, as well as increased p-SMAD1/5 relative to GFP controls (fig. S12, I to K).

To confirm that FXI overexpression activates BMP signaling to protect against diastolic dysfunction, we blocked the BMP receptor with the dorsomorphin homolog 1 (DMH1) (19). DMH1 is a selective inhibitor of activin receptor-like kinase 3, a type 1 BMP receptor. In NRVMs, DMH1 treatment suppressed SMAD1/5 phosphorylation induction by FXIa (fig. S13A). We also examined the effect of DMH1 in vivo. C57BL/6J mice were injected with AAV8-*F11* and fed with HFD + l-NAME for 7 weeks. Injection of DMH1 every other day to block SMAD1/5 phosphorylation (20) suppressed the change of body mass induced by FXI (fig. S13B), as well as the effect of FXI on p-SMAD1/5 levels, diastolic function, adipose

weight, blood cell numbers, and plasma cholesterol (Fig. 3, E to H, and fig. S13, C to G). These results confirmed that FXI protects against HFpEF by activating the BMP pathway.

FXI protease activity is required for the activation of BMP signaling

The FXI protein is conserved in human, mouse, rat, and other species and consists of four apple domains and one catalytic domain (fig. S14A). It is present in that plasma as a zymogen, which exists as a homodimer consisting of two identical polypeptide chains linked by disulfide bonds (fig. S14B) (21). During FXI activation, an internal peptide bond is cleaved by FXIIa (or XII) in each of the two chains, resulting in activated FXIa, a serine protease composed of two heavy and two light chains held together by disulfide bonds (fig. S14B). To test whether the catalytic domain is required for the function of FXI on the heart, we introduced two missense mutations in human and mouse FXI catalytic domains (fig. S14, A to E). These mutations were predicted to be exposed at the surface of the FXI molecule and to cause functional defects (type II mutation) (22). Next, we tested their function in vitro using a co-culture system. Huh7 human liver cells and AML12 mouse liver cells were transfected with respective human or mouse plasmids containing GFP control, wild-type (WT) *F11*, or *F11* with mutations. Then, cells were placed in co-cultures with NRVMs or 3T3-L1 adipocytes (fig. S15A). Twenty-four hours after transfection, FXI was highly induced in both Huh7 cells and AML12 cells (fig. S15B). In NRVMs, phosphorylation of SMAD1/5 was induced by WT FXI overexpression from both human and mouse liver cells, whereas mutant FXI did not exhibit a comparable effect (fig. S15C). By contrast, SMAD1/5 phosphorylation was not significantly ($P = 0.84$) induced by FXI in 3T3-L1 adipocytes, suggesting a heart-specific effect (fig. S15D). Consistent with phosphorylated SMAD1/5, *Col5a3* was decreased by WT FXI but not mutant FXI in NRVMs, indicating that the catalytic activity is required for its effect (fig. S15E).

To test the effect of missense mutation in vivo, we produced AAV8 with the mouse WT and mutant *F11* coding sequences. AAV8 containing *GFP* control, WT *F11*, and mutant *F11* (mF11-Mut2) was injected into C57BL/6J male mice followed by HFD + l-NAME for 7 weeks, after which plasma FXI was increased in FXI group and was comparable to the mutant FXI group (Fig. 3I and fig. S15F). Body weight and fat mass were decreased by WT FXI overexpression, but there was no significant difference ($P > 0.05$) between groups of mutant FXI and GFP controls (fig. S15, G to I), suggesting functional defects of mutant FXI. Consistently, the effects of FXI on p-SMAD1/5, heart weight, E/A ratio, E/e′ ratio, adipose weight, plasma cholesterol, and blood immune cells were not observed in mice carrying mutant FXI, demonstrating that catalytic activity is essential for the function of FXI in protecting against deleterious phenotypes in HFpEF (Fig. 3, J to M, and fig. S15, J to P).

FXI cleaves the BMP7 proprotein, activating the resulting growth factor fragment

As a serine protease, FXIa catalyzes the proteolysis of its substrates. BMP7 is synthesized as a large precursor molecule (inactive) that is cleaved to growth factor dimer or monomer (active) by proteolytic enzymes (23). We found that the cleavage site of the full-length BMP7 protein, at an arginine, is a common FXIa cleavage site (fig. S16, A and B) (24). We therefore hypothesized that BMP7 is a substrate of FXIa that mediates SMAD1/5 activation. FXI overexpression increased BMP7 growth factor dimer and monomer in the heart (Fig.

3N). Moreover, incubation of FXIa with BMP7 protein resulted in the cleavage of BMP7 (fig. S16C). Knocking down BMP7 or treatment with BMP7 antibody in NRVMs greatly reduced the activation of SMAD1/5 by FXIa (Fig. 3, O and P). The BMP7 protein is considerably enriched in heart tissue and cardiomyocytes (fig. S17), which may explain the preferential effect of FXI on the heart. The prodomain of BMP7 appears to bind to the extracellular matrix (23), suggesting that FXI cleaves the precursor BMP7 bound to the extracellular matrix in the heart; this then releases the dimer and monomer growth factors from the matrix to bind to the BMP receptor and activate SMAD1/5.

FXI knockout mice have reduced p-SMAD1/5 levels and increased diastolic dysfunction

We sought to further examine the cardioprotective effect of FXI using FXI knockout male mice in which the *F11* gene was disrupted by a PGK-neo cassette (25). F11 transcripts in the liver of heterozygous null mice (*F11*-Het) were reduced by ~50% compared with WT littermates (Fig. 4A). FXI was either absent or barely detectable in other tissues (Fig. 4A and fig. S4, A and B). Adult WT and *F11*-Het mice were then subjected to HFD + l-NAME for 7 weeks to induce HFpEF phenotypes. Compared with WT littermates on the HFpEF diet, p-SMAD1/5 was reduced in the hearts of *F11*-Het mice (Fig. 4B). Consistent with reduced p-SMAD1/5, *F11*-Het mice exhibited more severe diastolic dysfunction, as evidenced by the increased E/A ratio, E/e′ ratio, and LV mass but preserved ejection fraction (Fig. 4, C to G). Moreover, heart weight and lung weight were higher in *F11*-Het mice relative to WT controls, suggesting cardiac hypertrophy and lung congestion in FXI-deficient mice (Fig. 4, H and I). Exercise tolerance was also decreased in *F11*-Het mice compared with WT mice (Fig. 4J). By contrast, blood pressure was not significantly changed ($P > 0.05$) by FXI deficiency (fig. S18), indicating that FXI does not influence heart function through effects on blood pressure. These results collectively demonstrated the increased severity of diastolic dysfunction in FXI-deficient mice. We observed consistent effects of FXI in female mice with FXI heterozygous knockout (fig. S19).

FXI levels correlate with diastolic function in human cohorts

To determine the clinical relevance of FXI, we quantified plasma FXI in human patients with HFpEF and in normal participants. Plasma FXI protein was not significantly different ($P = 0.91$) between non–heart failure controls and HFpEF patients (Fig. 4K). However, plasma FXI was inversely correlated with E/e′ ratio in all participants (Fig. 4L), including HFpEF patients (Fig. 4M), supporting the conclusion that FXI protects against diastolic dysfunction in HFpEF.

Discussion

Our results indicate that liver-derived FXI specifically regulates cardiomyocytes through the BMP-SMAD1/5 pathway, resulting in attenuation of fibrosis, inflammation, and diastolic dysfunction in the context of an HFpEF model (Fig. 4N). Our analysis of diastolic function in a cohort of heart failure patients indicates the relevance of the pathway in humans and in mouse models, and the human GWAS results are consistent with that conclusion.

Prior studies have implicated the BMP and SMAD pathways in traits relevant to heart failure. It has been reported that the BMP pathway is enriched for HFpEF but not HFrEF (26). BMP2 has been found to alleviate heart failure with type 2 diabetes by inhibiting inflammasome formation (27), and is inversely correlated with the concentrations of atrial natriuretic peptide and brain natriuretic peptide in chronic heart failure patients with diabetes. Another study observed increased BMP6 in chronic heart failure patients, suggesting that BMP6 may be involved in the pathophysiology of systolic heart failure (28). In addition, SMAD1 protein was differentially expressed in a high-salt diet-induced HFpEF model (29).

FXI is a component of the intrinsic pathway of blood coagulation, acting downstream of FXII and functioning as a protease to activate FIX (14, 15, 21, 30, 31). Our data indicate that FXI overexpression also influences various systemic aspects of metabolism, and we cannot rule out the possibility that it may also affect organs other than the heart. FXI-deficient patients generally do not have spontaneous bleeding, because FXI is not required for the initial thrombin generation step (32), consistent with the possibility that it exhibits other previously unknown functions. Inactivating mutations of *F11* are relatively common among Ashkenazi Jews (33). A number of studies investigated the relationship between FXI and incident coronary heart disease, stroke, and ischemic cardiomyopathy (34, 35). FXI was reported to improve or protect against the inflammatory responses and cytokine responses to infections independently of its intrinsic coagulation activity (36-40).

The fact that FXI is a direct mediator of liver-heart communication suggests the possibility of using it in therapeutic applications for heart failure. It is important to note that elevated FXI is associated with various thromboses and ischemic stroke (41-43), so elevating FXI would be problematic as a therapeutic goal. However, the downstream BMP pathway could provide potential therapeutic targets.

Supplementary Material

Refer to Web version on PubMed Central for supplementary material.

ACKNOWLEDGMENTS

Funding: This work was supported by the National Institutes of Health (grants DK120342 and HL147883; grants HL138193, DK130640, and DK097771 to M.M.S.; grants R01HL133169 and R01HL148110 to H.A.; and grant DK125354 to Z.Z.).

REFERENCES AND NOTES

1. Friedman JM, Halaas JL, Nature 395, 763–770 (1998). [PubMed: 9796811]
2. Møller S, Bernardi M, Eur. Heart J 34, 2804–2811 (2013). [PubMed: 23853073]
3. Baskin KK, Bookout AL, Olson EN, EMBO Mol. Med 6, 436–438 (2014). [PubMed: 24623378]
4. Packer M, Am. J. Med 133, 170–177 (2020). [PubMed: 31622581]
5. Pacifico L et al., Hepatology 59, 461–470 (2014). [PubMed: 23843206]
6. Cao Y et al., Circulation 145, 1102–1104 (2022). [PubMed: 35377742]
7. Dunlay SM, Roger VL, Redfield MM, Nat. Rev. Cardiol 14, 591–602 (2017). [PubMed: 28492288]
8. Hogg K, Swedberg K, McMurray J, J. Am. Coll. Cardiol 43, 317–327 (2004). [PubMed: 15013109]

9. Owan TE et al., N. Engl. J. Med 355, 251–259 (2006). [PubMed: 16855265]
10. Seldin MM et al., Cell Metab. 27, 1138–1155.e6 (2018). [PubMed: 29719227]
11. Lusis AJ et al., J. Lipid Res 57, 925–942 (2016). [PubMed: 27099397]
12. Gandhi PU et al., JACC Heart Fail. 4, 860–869 (2016). [PubMed: 27744089]
13. Schiattarella GG et al., Nature 568, 351–356 (2019). [PubMed: 30971818]
14. Walsh PN, Thromb. Haemost 86, 75–82 (2001). [PubMed: 11487044]
15. Emsley J, McEwan PA, Gailani D, Blood 115, 2569–2577 (2010). [PubMed: 20110423]
16. Ferkingstad E et al., Nat. Genet 53, 1712–1721 (2021). [PubMed: 34857953]
17. Kandis H et al., Emerg. Med. J 28, 575–578 (2011). [PubMed: 20660896]
18. Withaar C et al., Cardiovasc. Res 117, 2108–2124 (2021). [PubMed: 32871009]
19. Petersen MA et al., Neuron 96, 1003–1012.e7 (2017). [PubMed: 29103804]
20. Shan Y et al., Front. Neurosci 12, 964 (2018). [PubMed: 30618586]
21. Fujikawa K, Chung DW, Hendrickson LE, Davie EW, Biochemistry 25, 2417–2424 (1986). [PubMed: 3636155]
22. Saunders RE et al., Thromb. Haemost 102, 287–301 (2009). [PubMed: 19652879]
23. Gregory KE et al., J. Biol. Chem 280, 27970–27980 (2005). [PubMed: 15929982]
24. Ge X et al., Blood 131, 353–364 (2018). [PubMed: 29158361]
25. Gailani D, Lasky NM, Broze GJ Jr., Blood Coagul. Fibrinolysis 8, 134–144 (1997). [PubMed: 9518045]
26. Adamo L et al., J. Am. Coll. Cardiol 76, 1982–1994 (2020). [PubMed: 33092734]
27. Zhang JM et al., Exp. Ther. Med 22, 897 (2021). [PubMed: 34257710]
28. Banach J et al., Clin. Exp. Pharmacol. Physiol 43, 1247–1250 (2016). [PubMed: 27592865]
29. Zhou G et al., Front. Physiol 12, 607089 (2021). [PubMed: 34721049]
30. Wu W et al., J. Biol. Chem 283, 18655–18664 (2008). [PubMed: 18441012]
31. Bolton-Maggs PH, Baillieres Clin. Haematol 9, 355–368 (1996). [PubMed: 8800510]
32. Wheeler AP, Gailani D, Expert Rev. Hematol 9, 629–637 (2016). [PubMed: 27216469]
33. Asakai R, Chung DW, Davie EW, Seligsohn U, N. Engl. J. Med 325, 153–158 (1991). [PubMed: 2052060]
34. Appiah D et al., Blood Coagul. Fibrinolysis 28, 389–392 (2017). [PubMed: 28009647]
35. Zabczyk M, Butenas S, Palka I, Nessler J, Undas A, Pol. Arch. Med. Wewn 120, 334–340 (2010). [PubMed: 20864906]
36. Stroo I et al., Thromb. Haemost 117, 1601–1614 (2017). [PubMed: 28492700]
37. Ngo ATP et al., J. Thromb. Haemost 19, 1001–1017 (2021). [PubMed: 33421301]
38. Puy C et al., J. Immunol 206, 1784–1792 (2021). [PubMed: 33811105]
39. Tucker EI et al., Blood 119, 4762–4768 (2012). [PubMed: 22442348]
40. Bane CE Jr. et al., PLOS ONE 11, e0152968 (2016). [PubMed: 27046148]
41. Rovite V et al., Thromb. Res 134, 659–663 (2014). [PubMed: 25091233]
42. Li Y et al., J. Thromb. Haemost 7, 1802–1808 (2009). [PubMed: 19583818]
43. Chong M et al., Circulation 140, 819–830 (2019). [PubMed: 31208196]
44. Pan C, R script used to perform the volcano plots and PCA plot (F11_SF7) for: Cao Y et al., Liver-heart cross-talk mediated by coagulation factor XI protects against heart failure, Zenodo (2022); 10.5281/zenodo.6961041.

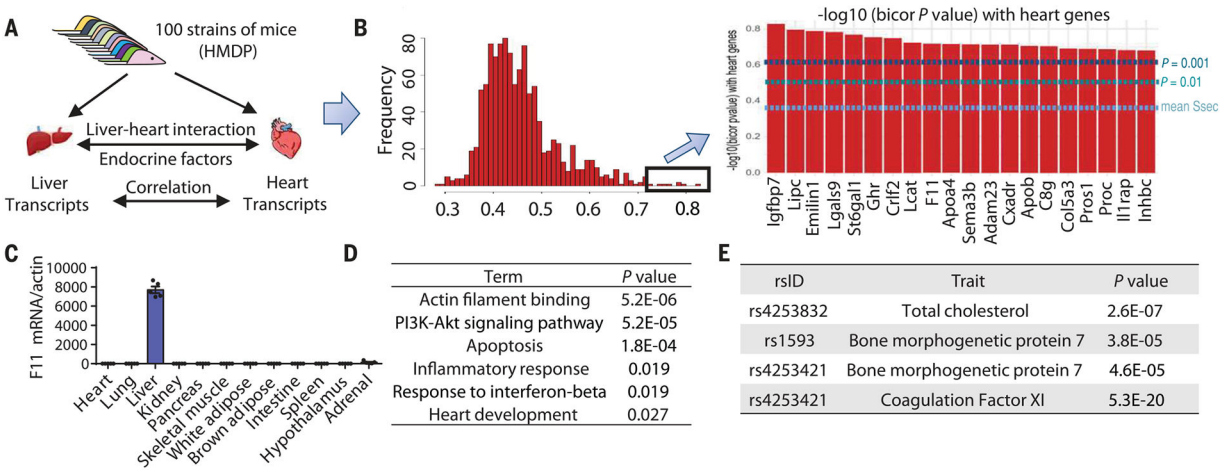

D

Term	*P* value
Actin filament binding	5.2E-06
PI3K-Akt signaling pathway	5.2E-05
Apoptosis	1.8E-04
Inflammatory response	0.019
Response to interferon-beta	0.019
Heart development	0.027

E

rsID	Trait	*P* value
rs4253832	Total cholesterol	2.6E-07
rs1593	Bone morphogenetic protein 7	3.8E-05
rs4253421	Bone morphogenetic protein 7	4.6E-05
rs4253421	Coagulation Factor XI	5.3E-20

Fig. 1. Systems genetics analysis of cross-tissue correlations identifies proteins mediating liver-heart cross-talk.

(**A**) Schematic illustrating the identification of the liver-heart interaction using 100 inbred strains of mice (HMDP). The correlation between the secreted factors (from the liver) and cardiac gene expression (RNA-Seq) was used for liver-heart predictions. This framework identified peptides secreted by the liver and strongly associated with the cardiac gene network. $n = 4$ to 20 mice for each strain. (**B**) Distribution of significance score for all liver genes across all heart gene expression in 100 strains (left). List shows the top 20 genes potentially mediating liver-heart communication (right). (**C**) Quantitative reverse transcription polymerase chain reaction (qRT-PCR) analysis of *F11* expression across indicated tissues in C57BL/6J mice ($n = 4$). All data are presented as means ± SEM. (**D**) Pathway enrichment derived from heart genes correlated with liver *F11* expression. (**E**) GWAS loci for indicated clinical traits in human populations. The GWAS catalog and PhenoScanner databases consist of human genotype-phenotype associations from publicly available genetic association studies.

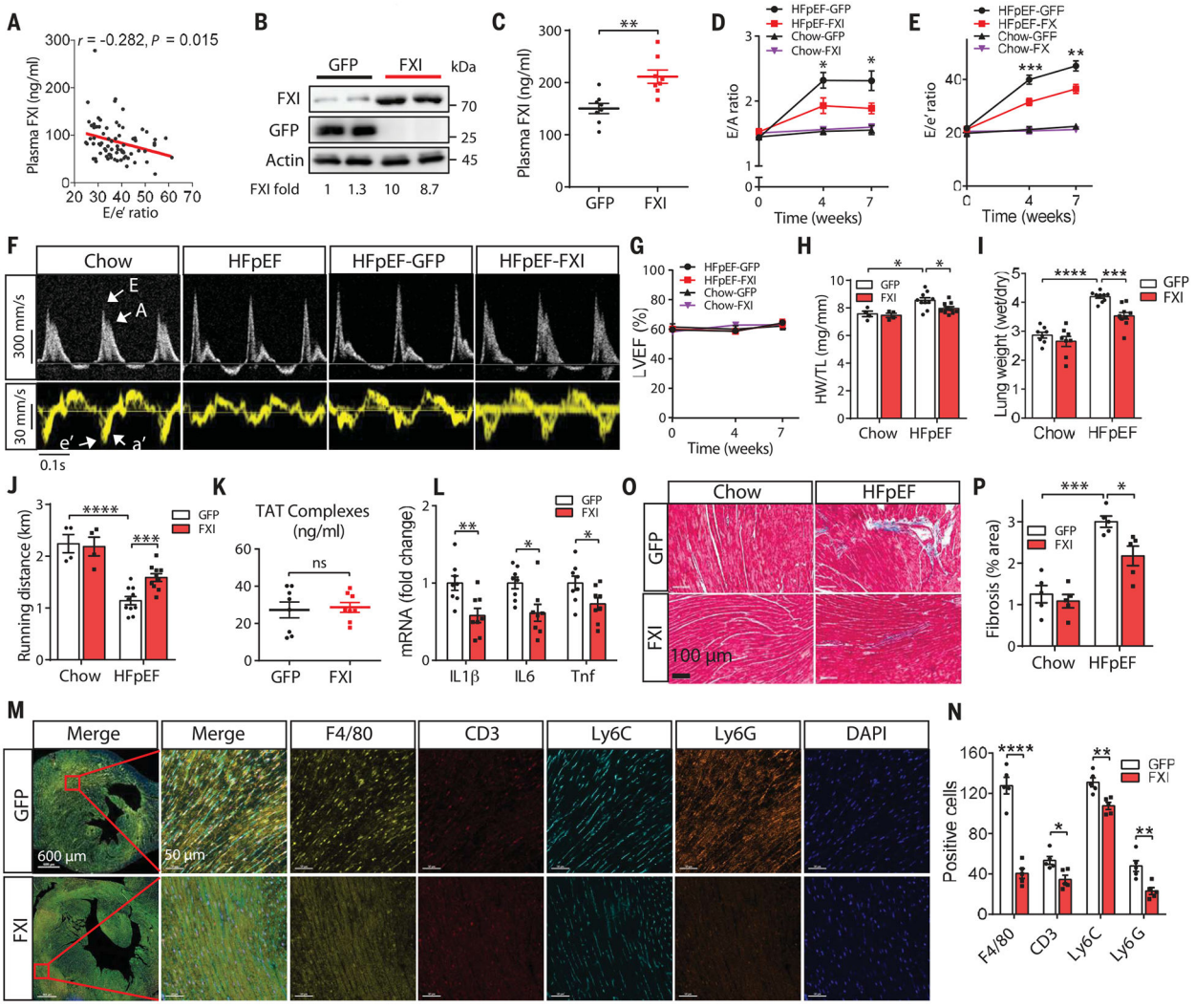

Fig. 2. FXI overexpression reverses HFpEF-induced diastolic dysfunction, inflammation, and fibrosis.

(**A**) Thirty inbred strains of male mice were subjected to HFD + l-NAME to induce HFpEF. Plasma FXI concentrations and diastolic function (E/e′ ratio) were assessed after 7 weeks of feeding. Plasma FXI concentrations were inversely correlated with diastolic dysfunction. (**B** to **L**) C57BL/6J male mice were injected with AAV8 containing the cDNA sequence for *GFP* or *F11* and then fed with HFD + l-NAME for 7 weeks. Western blotting shows liver FXI protein (B), plasma FXI concentrations (C), E/A ratio (D), E/e′ ratio (E), representative images of echocardiography (F), LVEF (G), heart weight/tibia length ratio (H), lung weight [wet/dry ratio (I)], running distance (J), thrombin-antithrombin complexes [TAT (K)], and relative mRNA expression of indicated genes in the heart (L). $n = 4$ for chow in (D) to (H); in other panels, $n = 8$ to 10. (**M** and **N**) C57BL/6J male mice injected with AAV8-*GFP* or AAV8-*F11* were on HFD + l-NAME for 7 weeks ($n = 5$). Representative images of immunohistochemistry staining (M) and quantification of positive cells (N) showing inflammatory cell infiltration in the heart tissue. (**O** and **P**) C57BL/6J male mice injected with AAV8-*GFP* or AAV8-*F11* were given a chow diet or HFD + l-NAME for 7 weeks (*n*

= 5). Representative images of Masson's trichrome staining (O) and quantification (P) show fibrosis in the heart tissue. Each point represents a mouse. All data are presented as means ± SEM. ns, not significant. *$P < 0.05$, **$P < 0.01$, ***$P < 0.001$, and ****$P < 0.0001$ by two-way ANOVA [(D) to (J) and (P)] or by Student's *t* test [(B) and (C) and (K) to (N)]. For (A) to (C) and (K) to (N), all mice were on HFD + l-NAME. LYM, lymphocytes; MONO, monocytes; GRAN, granulocytes.

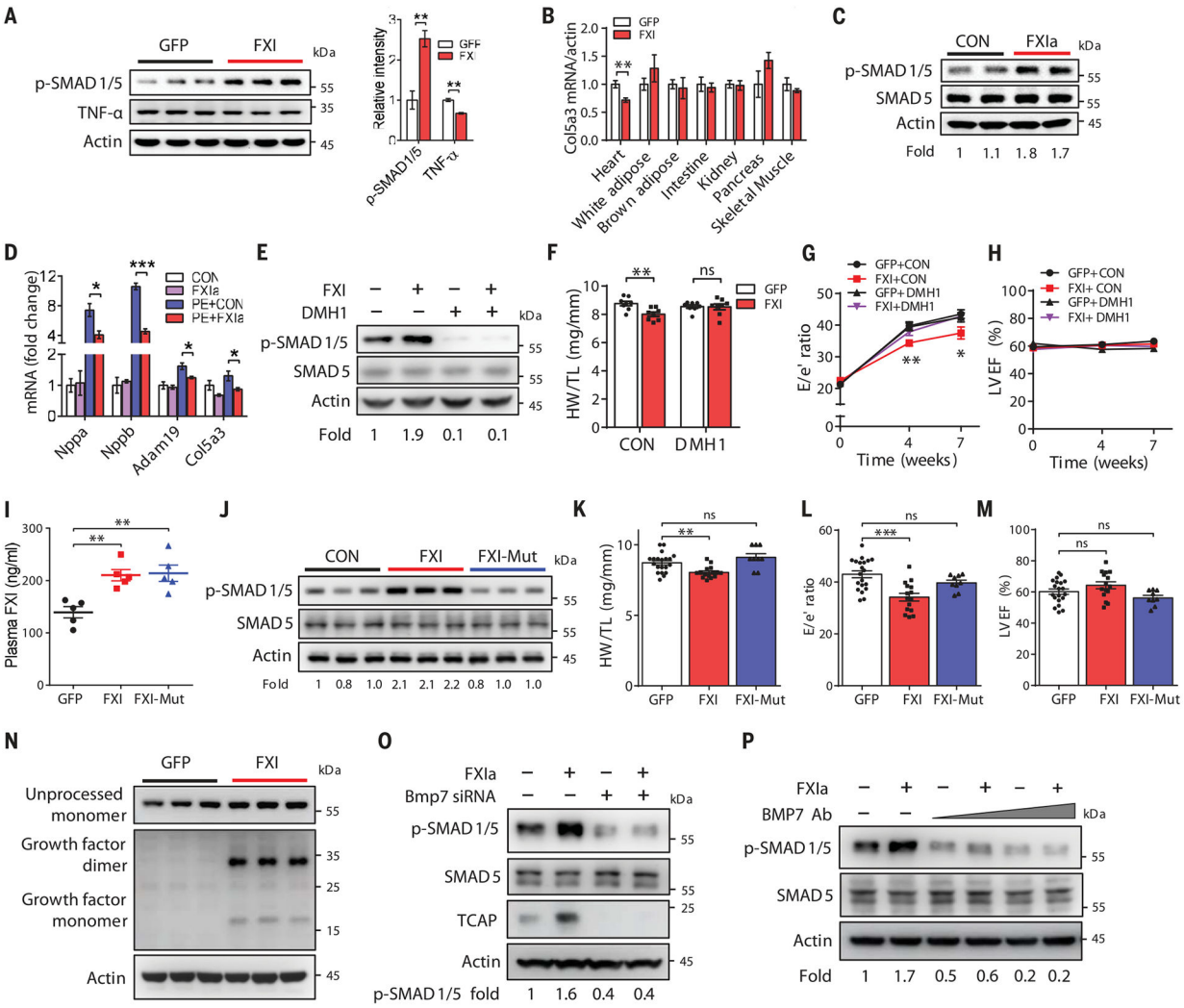

Fig. 3. FXI activates BMP-SMAD1/5 pathway in the heart.

(**A**) Western blotting and quantification showing protein levels in heart tissue from C57BL/6J male mice injected with AAV8-*GFP* or AAV8-*F11* and fed with 7 weeks of HFD + l-NAME. Actin served as the loading control. $n = 5$. (**B**) qRT-PCR analysis showing the mRNA levels of *Col5a3* in the indicated tissue from C57BL/6J male mice injected with AAV8-*GFP* or AAV8-*F11* and fed HFD + l-NAME for 7 weeks. Heart, $P < 0.001$; others, not significant. $n = 8$. (**C** and **D**) NRVMs were treated with control or human FXIa protein (1 μg/ml) with medium containing control or phenylephrine (PE, 100 μM) for 24 hours. p-SMAD1/5 (C) and the indicated genes (D) were examined. Actin served as the loading control. $n = 6$. (**E** to **H**) C57BL/6J male mice were injected with AAV8-*GFP* or AAV8-*F11* with DMH1 and fed with HFD + l-NAME for 7 weeks. Heart p-SMAD1/5 level (E), heart weight/tibia length ratio (F), E/e′ ratio (G), and LVEF (H) were determined. $n = 3$ for (E) and $n = 8$ for (F) to (H). (**I** to **M**) C57BL/6J male mice were injected with AAV8-*GFP*, AAV8-*F11*, or AAV8-*F11*-Mut (m*F11*-Mut2) and fed with HFD + l-NAME for 7 weeks. Plasma FXI levels (I), heart p-SMAD1/5 protein level (J), heart weight/tibia length ratio (K), E/e′ ratio (L), and LVEF (M) were measured. $n = 5$ for (I), $n = 6$ for

(J), and n = 10 to 20 for (K) to (M). (**N**) C57BL/6J male mice were injected with either AAV8-*GFP* or AAV8-*F11* and then fed with HFD + l-NAME for 7 weeks. BMP7 proteins in unprocessed monomer, growth factor dimer, and monomer under nonreducing condition were determined. (**O**) NRVMs were treated with control or human FXIa protein (1 μg/ml) plus negative control or Bmp7 siRNA with medium containing PE (100 μM) for 24 hours. p-SMAD1/5 and Tcap proteins were examined. Actin served as the loading control. n = 3. (**P**) NRVMs were treated with control or human FXIa protein (1 μg/ml), BMP7 antibody (no antibody control, 1:100 and 1:50), with medium containing PE (100 μM) for 2 hours, and the p-SMAD1/5 level was determined. Actin served as the loading control. n = 4. Each point represents a mouse. All data are presented as means ± SEM. ns, not significant. *P < 0.05, **P < 0.01, and ***P < 0.001 by two-way ANOVA [(D) to (H)], one-way ANOVA [(I) to (M)], or Student's t test [(A) to (C)].

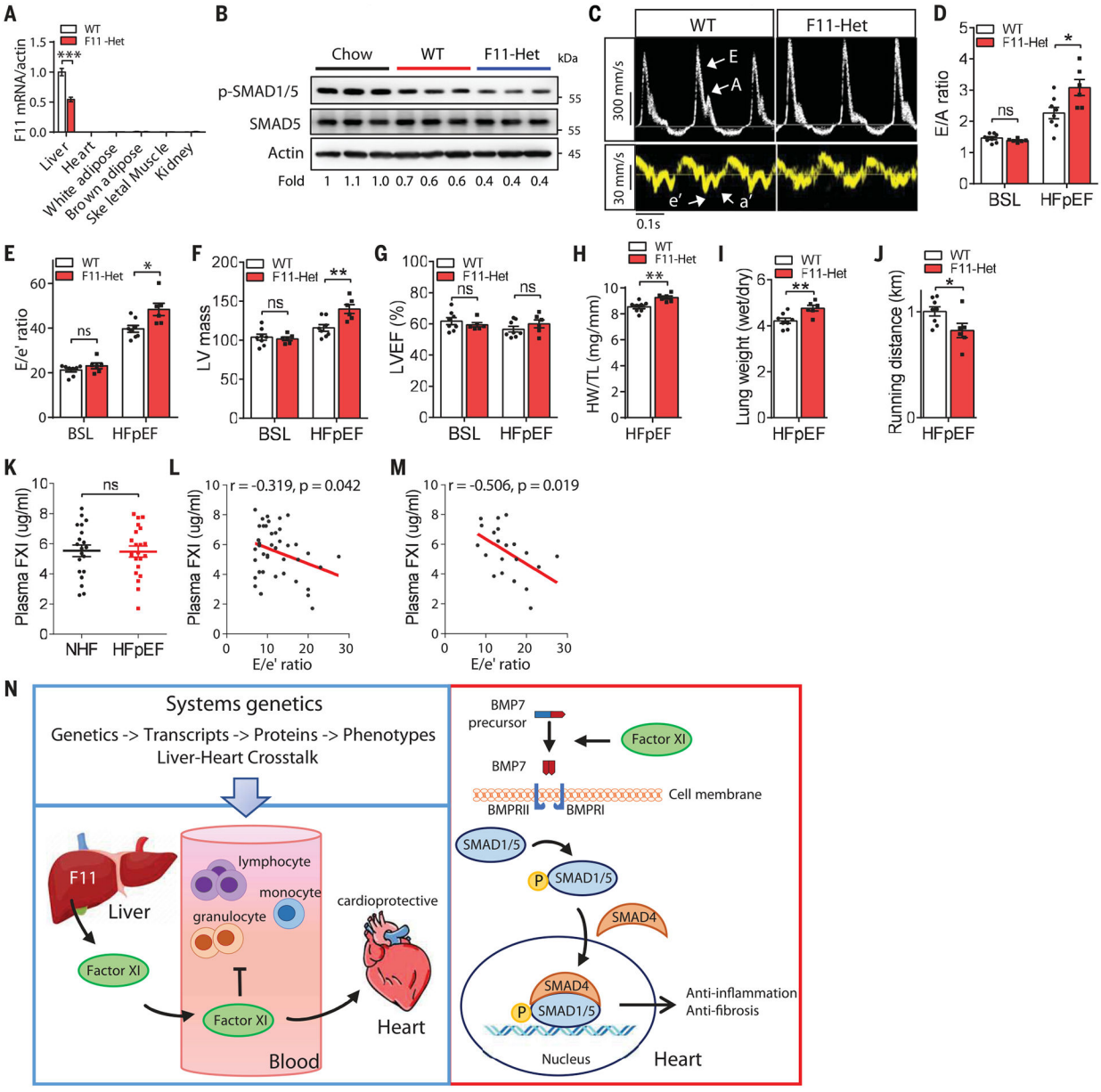

Fig. 4. Reduced FXI concentrations are associated with diastolic dysfunction in mice and humans.

Heterozygous B6.129X1-F11^{tm1Gjb}/J (*F11*-Het) mice and WT littermates at 8 weeks of age were subjected to HFD + l-NAME for 7 weeks. $n = 8$ for WT and $n = 6$ for *F11*-Het. (**A**) qRT-PCR showing *F11* mRNA in the indicated tissues from WT and *F11*-Het mice. $n = 4$. (**B**) Western blotting showing p-SMAD1/5 in the hearts of WT mice fed with chow diet (Chow), WT, and *F11*-Het mice fed with HFD + l-NAME for 7 weeks. $n = 5$. (**C** to **G**) Representative images of echocardiography (C), E/A ratio (D), E/e′ ratio (E), LV mass (F), and LVEF (G) were examined at baseline (BSL) and after 7 weeks of HFD + l-NAME feeding (HFpEF). $n = 8$ for WT and $n = 6$ for *F11*-Het. (**H** to **J**) Heart weight/tibia length ratio (H), lung weight [wet/dry ratio (I)], and running distance (J) were examined after 7 weeks of HFD + l-NAME feeding (HFpEF). $n = 8$ for WT

and $n = 6$ for *F11*-Het. (**K**) Plasma FXI protein in non-HFpEF controls (NHF, $n = 20$) and HFpEF patients ($n = 21$). (**L** and **M**) Plasma FXI protein was inversely correlated with E/e′ ratio in all participants (L), including HFpEF patients (M). (**N**) Illustration summarizing FXI-mediated liver-heart cross-talk in protecting against heart failure. Using a bioinformatic framework that integrates global liver-heart transcriptome and cardiometabolic trait data from the HMDP, we found that coagulation FXI, secreted by the liver, exhibits cardioprotective effects on the progression of HFpEF. FXI overexpression in the liver mitigates the diastolic dysfunction, inflammation, and fibrosis induced by HFpEF. FXIa cleaves the BMP7 precursor and activates the BMP7-SMAD1/5 pathway in the heart to mediate the anti-inflammatory and anti-fibrotic effects. Each point represents a mouse. All data are presented as means ± SEM. ns, not significant. $*P < 0.05$, $**P < 0.01$, and $***P < 0.001$ by two-way ANOVA [(D) to (G)], one-way ANOVA (B), or Student's *t* test [(A) and (H) to (K)].